Diverse Pathways of Activation and Deactivation of Half-Sandwich Aryloxide Titanium Polymerization Catalysts

Khamphee Phomphrai,*[,†,‡] Andrew E. Fenwick,[†] Shalini Sharma,[†] Phillip E. Fanwick,[†] James M. Caruthers,[§] W. Nicholas Delgass,[§] Mahdi M. Abu-Omar,*[,†] and Ian P. Rothwell[†,⊥]

Department of Chemistry and Center for Catalyst Design and School of Chemical Engineering and Center for Catalyst Design, Purdue University, 560 Oval Drive, West Lafayette, Indiana 47907-2084

Received August 22, 2005

A series of half-sandwich aryloxide titanium complexes, [CpTi(OAr)Me_2] (Cp = C_5H_5; OAr = OC_6H_3-Me_2-2,6, $OC_6H_3Et_2$-2,6, $OC_6H_3{}^iPr_2$-2,6, $OC_6H_3{}^tBu_2$-2,6, and OC_6HPh_4-2,3,5,6), have been synthesized. These compounds react with $B(C_6F_5)_3$ to give thermally unstable complexes [CpTi(OAr)Me][$MeB(C_6F_5)_3$]. Two different deactivation pathways have been identified within the series. The tetraphenylphenoxide cationic methyl compound decomposes cleanly at room temperature to give [CpTi(OC_6HPh_4-2,3,5,6)-(C_6F_5){$CH_2B(C_6F_5)_2$}] and methane with a first-order rate constant of 7.6(2) × 10^{-4} s^{-1} at 25 °C. For relatively smaller aryloxide ligands, OAr = $OC_6H_3{}^iPr_2$-2,6, $OC_6H_3{}^tBu_2$-2,6, a Me/C_6F_5 exchange takes place, yielding CpTi(OAr)Me(C_6F_5) and $MeB(C_6F_5)_2$. The cationic titanium complexes are shown to be active for the polymerization of 1-hexene. At −20 and 0 °C, first-order dependence on the concentration of 1-hexene is observed. The rate of polymerization decreases with increasing steric hindrance of aryloxides except for OAr = OC_6HPh_4-2,3,5,6.

Introduction

A great degree of success has been reported in the area of group 4 metallocenes as olefin polymerization catalyst precursors.[1,2] The cationic complexes $[Cp_2MCH_3]^+$ (M = Ti, Zr, Hf),[3] generated from the activation of dihalide or dialkyl complexes with a varieties of activators[4] such as MAO, perfluoroaryl boranes, $B(C_6F_5)_3$, or $[Ph_3C][B(C_6F_5)_4]$, have been shown to be catalytically active in olefin polymerization. In contrast to the heterogeneous Ziegler−Natta catalysts, a well-defined coordination environment in the homogeneous metallocenes afforded in many instances "single-site" catalysts, which led to an efficient control of polymer properties such as molecular weight, molecular weight distribution, stereochemical microstructure, and comonomer incorporation, through systematic ligand modification.[1,5]

Following the success of group 4 metallocene chemistry, there has been a great interest in the development of related homogeneous catalysts supported by non-Cp ancillary ligands.[6−10] These include constrained geometry,[11] half-sandwich complexes bearing pendant electron donors[12,13] and related diamide[7a−d,i,j]

* Corresponding authors. E-mail: sckpp@mahidol.ac.th; mabuomar@purdue.edu.

† Department of Chemistry and Center for Catalyst Design.

‡ Present address: Department of Chemistry, Faculty of Science, Mahidol University, Rama 6 Road, Bangkok 10400, Thailand.

§ School of Chemical Engineering and Center for Catalyst Design.

⊥ This paper is dedicated to the memory of our mentor, colleague, and friend Ian P. Rothwell, Richard B. Moore Distinguished Professor of Chemistry.

(1) (a) Alt, H. G.; Köppl, A. *Chem. Rev.* **2000**, *100*, 1205−1221. (b) Coates, G. W. *Chem. Rev.* **2000**, *100*, 1223−1252. (c) Resconi, L.; Cavallo, L.; Fait, A.; Piemontesi, F. *Chem. Rev.* **2000**, *100*, 1253−1345. (d) Coates, G. W. *J. Chem. Soc., Dalton Trans.* **2002**, 467−475.

(2) (a) Bochmann, M. *J. Chem. Soc., Dalton Trans*. **1996**, 255. (b) Brintzinger, H.-H.; Fischer, D.; Mülhaupt, R.; Rieger, B.; Waymouth, R. M. *Angew. Chem., Int. Ed. Engl.* **1995**, *34*, 1143. (c) Möhring, P. C.; Coville, N. J. *J. Organomet. Chem*. **1994**, *479*, 1. (d) Kaminsky, W.; Kulper, K.; Brintzinger, H. H. *Angew. Chem., Int. Ed. Engl*. **1985**, *24*, 507.

(3) Yang, X. M.; Stern, C. L.; Marks, T. J. *J. Am. Chem. Soc.* **1994**, *116*, 10015−10031.

(4) Chen, E. Y. X.; Marks, T. J. *Chem. Rev.* **2000**, *100*, 1391−1434.

(5) Corradini, P.; Guerra, G.; Cavallo, L. *Acc. Chem. Res.* **2004**, *37*, 231−241.

(6) (a) Britovsek, G. J. P.; Gibson, V. C.; Wass, D. F. *Angew. Chem., Int. Ed.* **1999**, *38*, 428−447. (b) Coates, G. W.; Hustad, P. D.; Reinartz, S. *Angew. Chem., Int. Ed.* **2002**, *41*, 2236−2257. (c) Gibson, V. C.; Spitzmesser, S. K. *Chem. Rev.* **2003**, *103*, 283−315.

(7) (a) Scollard, J. D.; McConville, D. H. *J. Am. Chem. Soc*. **1996**, *118*, 10008. (b) Tsuie, B.; Swenson, D. C.; Jordan, R. F.; Petersen, J. L. *Organometallics* **1997**, *16*, 1392. (c) Scollard, J. D.; McConville, D. H.; Rettig, S. J. *Organometallics* **1997**, *16*, 1810. (d) Baumann, R.; Davis, W. M.; Schrock, R. R. *J. Am. Chem. Soc*. **1997**, 119, 3830. (e) Gömez, R.; Green, M. L. H.; Haggitt, J. L. *J. Chem. Soc., Chem. Commun*. **1994**, 2607. (f) Friedrich, S.; Gade, L. H.; Edwards, A. J.; McPartlin, M. *J. Chem. Soc., Dalton Trans*. **1993**, 2861. (g) Brand, H.; Capriotti, J. A.; Arnold, J. *Organometallics* **1994**, *13*, 4469. (h) Aoyagi, K.; Gantzel, P. K.; Kalai, K.; Tilley, T. D. *Organometallics* **1996**, *15*, 923. (i) Cloke, F. G. N.; Geldbach, T. J.; Hitchcock, P. B.; Love, J. B. *J. Organomet. Chem*. **1996**, *506*, 343. (j) Jeon, Y.-M.; Park, S. J.; Heo, J.; Kim, K. *Organometallics* **1998**, *17*, 3161. (k) Horton, A. D.; de With, J.; van der Linden, A. J.; van de Weg, H. *Organometallics* **1996**, *15*, 2672. (l) Shah, S. A. A.; Dorn, H.; Voigt, A.; Roesky, H. W.; Parisini, E.; Schmidt, H.-G.; Noltemeyer, M. *Organometallics* **1996**, *15*, 3176. (m) Herskovics-Korine, D.; Eisen, M. S. *J. Organomet. Chem*. **1995**, *503*, 307.

(8) (a) van der Linden, A.; Schaverien, C. J.; Meijboom, N.; Grant, C.; Orpen, A. G. *J. Am. Chem. Soc.* **1995**, *117*, 3008. (b) Fokken, S.; Spaniol, T. P.; Kang, H.-C.; Massa, W.; Okuda, J. *Organometallics* **1996**, *15*, 5069. (c) For cationic zirconium alkyls supported by chelating phenoxides see: Cozzi, P. G.; Gallo, E.; Floriani, C.; Chiesi-Villa, A.; Rizzoli, C. *Organometallics* **1995**, *14*, 4994.

(9) Groysman, S.; Goldberg, I.; Kol, M. *Organometallics* **2003**, *22*, 3015, and references therein.

(10) (a) Schrock, R. R.; Adamchuk, J.; Ruhland, K.; Lopez, L. P. H. *Organometallics* **2005**, *24*, 857−866. (b) Schrock, R. R.; Baumann, R.; Reid, S. M.; Goodman, J. T.; Stumpf, R.; Davis, W. M. *Organometallics* **1999**, *18*, 3649−3670. (c) Goodman, J. T.; Schrock, R. R. *Organometallics* **2001**, *20*, 5205−5211. (d) Schrodi, Y.; Schrock, R. R.; Bonitatebus, P. J., Jr. *Organometallics* **2001**, *20*, 3560−3573.

(11) (a) Devore, D. D.; Timmers, F. J.; Hasha, D. L.; Rosen, R. K.; Marks, T. J.; Deck, P. A.; Stern, C. L. *Organometallics* **1995**, *14*, 3132. (b) Chen, Y.-X.; Marks, T. J. *Organometallics* **1997**, *16*, 3649. (c) Duda, L.; Erker, G.; Frohlich, R.; Zippel, F. *Eur. J. Inorg. Chem*. **1998**, 1153. (d) Blais, M. S.; Chien, J. C. W.; Rausch, M. D. *Organometallics* **1998**, *17*, 3775.

(12) Siemeling, U. *Chem. Rev.* **2000**, *100*, 1495−1526.

(13) Butenschon, H. *Chem. Rev.* **2000**, *100*, 1527−1564.

10.1021/om0507272 CCC: $33.50
Publication on Web 11/25/2005

based catalyst systems. Other catalysts based on aryloxide[8,9,14,15] and alkoxide[16] ligands have also received some attention recently. The aryloxide ligand can adopt a bonding motif isolobal with that of the cyclopentadienyl ligand, potentially bonding in a $o^2\pi^4$ fashion. A key property of these ligands is their tunability, as a wide collection of phenols offering a unique and diverse set of steric and electronic features are commercially available or can be readily synthesized. We have reported on a series of bisaryloxide complexes $(ArO)_2MR_2$ (M = Ti, Zr; R = Me, CH_2Ph).[17] Although the bisaryloxide complexes can be activated with $B(C_6F_5)_3$, giving compounds $[(ArO)_2MR][RB(C_6F_5)_3]$, they showed very moderate catalytic activity for the polymerization of ethylene, propylene, and 1-hexene.[17b] On the other hand, the polymerization activity is dramatically enhanced when one aryloxide ligand is replaced by one cyclopentadienyl ligand. From a series of studies, Nomura and co-workers have shown that mixed Cp/aryloxide titanium complexes $CpTi(OAr)Cl_2$ are highly active for 1-hexene, ethylene, styrene, and propylene polymerization when activated with methylaluminoxane (MAO).[15]

While the dihalide derivatives, $CpTi(OAr)X_2$, have been studied extensively with a large excess of MAO in olefin polymerization, studies on the dialkyl analogues $CpTi(OAr)R_2$ until now have been very minimal.[18,19] Activation of $CpTi(OAr)R_2$ with 1 equiv of activator such as $B(C_6F_5)_3$ or $[Ph_3C][B(C_6F_5)_4]$ would eliminate the need for excess MAO or trialkylaluminum as required for the dihalide complexes, thus making the catalyst system less complicated and amenable to quantitative rate measurements. In this study, we report on the synthesis of a series of dialkyl $CpTi(OAr)R_2$ complexes along with their activation, deactivation, and olefin polymerization kinetics.

Results and Discussion

Synthesis and Characterization of Dimethyl Compounds. A series of compounds $CpTi(OAr)Me_2$, where Cp = C_5H_5; OAr = $OC_6H_3Me_2$-2,6 (**1**), $OC_6H_3Et_2$-2,6 (**2**), $OC_6H_3{}^iPr_2$-2,6 (**3**), $OC_6H_3{}^tBu_2$-2,6 (**4**), and OC_6HPh_4-2,3,5,6 (**5**), have been synthesized. We previously reported the syntheses of compounds **1**, **3**, and **5**.[18] Starting from $CpTiCl_3$, $[CpTiMe_3]$ was prepared in situ by reacting with 3 equiv of LiMe at −78 °C, followed by addition of the corresponding phenol, giving **1**−**3** and **5** in high yield and purity (Scheme 1, method A).[18] However, the deprotonation of $HOC_6H_3{}^tBu_2$-2,6 by $[CpTiMe_3]$ was not successful due to the steric bulk of ^{t}Bu groups. Thus, compound **4** was prepared from the reaction of $CpTiCl_3$ with $LiOC_6H_3{}^tBu_2$-2,6 to give $CpTi(OC_6H_3{}^tBu_2\text{-}2,6)Cl_2$,[20] followed by methylation with 2 equiv of LiMe (Scheme 1, method B). Spectroscopic characterization of **1**−**5** did not reveal remarkable features that were not anticipated. ^{1}H NMR of Ti-*Me* groups shift downfield (δ 0.91, 0.91, 0.94, and 1.02 ppm) with increasing alkyl size from Me to ^{t}Bu in **1**−**4**. For relatively small aryloxide ligands, compounds **1**−**3** are not stable at room temperature, where a slow decomposition was observed over days to produce $CpTi(OAr)_2Me$.[18] Compounds **4** and **5** are stable at room temperature over 1 month in a drybox.

Scheme 1

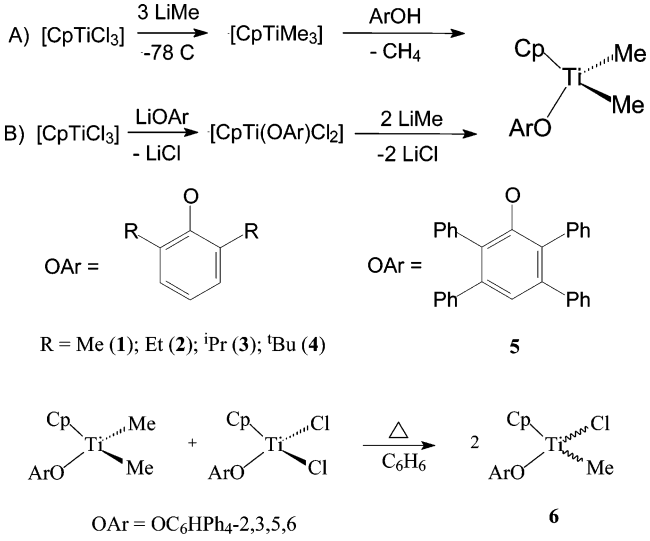

Heating a solution of $CpTi(OC_6HPh_4\text{-}2,3,5,6)Cl_2$ and the dimethyl compound **5** in benzene gave the mixed monomethyl/monochloro $CpTi(OC_6HPh_4\text{-}2,3,5,6)(Cl)(Me)$, **6**, in quantitative yield (Scheme 1). A similar comproportionation of the dichloride and dimethyl titanium complexes to give mixed monomethyl/monochloro titanium complexes has been documented.[21] The preparation, an ORTEP drawing of the molecular structure of **6**, and selected bond distances (Å) and angles (deg) are given in the Supporting Information.

Synthesis and Deactivation of Cationic Titanium Methyl Complexes. Addition of 1 equiv of $B(C_6F_5)_3$ to the dimethyl compounds **1**−**5** in benzene or toluene led to the immediate formation of the thermally unstable (vide infra) cationic methyl compounds **7**−**11** as indicated by ^{1}H NMR and an instant color change from yellow to red (Scheme 2). At −25 °C, ^{1}H NMR of compounds **7**−**11** showed a single set of Cp and OAr resonances along with resolved Ti-*Me* (sharp) and Ti-*Me*-B (broad) signals. The Ti-*Me* proton signals shifted $\Delta\delta$ 0.60−0.74 ppm downfield from their neutral parent dimethyl complexes. The Ti-*Me* proton signals also shifted downfield (δ 1.51, 1.57, 1.61, and 1.76 ppm) with increasing size of alkyl groups

(14) (a) Thorn, M. G.; Fanwick, P. E.; Chesnut, R. W.; Rothwell, I. P. *Chem. Commun.* **1999**, 2543. (b) Turner, L. E.; Thorn, M. G.; Fanwick, P. E.; Rothwell, I. P. *Chem. Commun.* **2003**, 1034. (c) Thorn, M. G.; Parker, J. R.; Fanwick, P. E.; Rothwell, I. P. *Organometallics* **2003**, *22*, 4658. (d) Turner, L. E.; Swartz, R. D.; Thorn, M. G.; Chesnut, R. W.; Fanwick, P. E.; Rothwell, I. P. *Dalton Trans.* **2003**, 4580. (e) Turner, L. E.; Thorn, M. G.; Fanwick, P. E.; Rothwell, I. P. *Organometallics* **2004**, *23*, 1576.

(15) (a) Nomura, K.; Okumura, H.; Komatsu, T.; Naga, N. *Macromolecules* **2002**, *35*, 5388−5395. (b) Nomura, K.; Oya, K.; Imanishi Y. *J. Mol. Catal. A* **2001**, *174*, 127−140. (c) Nomura, K.; Fudo, A. *Catal. Commun.* **2003**, *4*, 269−274. (d) Nomura, K.; Tsubota, M.; Fujiki, M. *Macromolecules* **2003**, *36*, 3797−3799. (e) Nomura, K.; Fudo, A. *Inorg. Chim. Acta* **2003**, *345*, 37−43. (f) Nomura, K.; Okumura, H.; Komatsu, T.; Naga, N.; Imanishi, Y. *J. Mol. Catal. A* **2002**, *190*, 225−234. (g) Nomura, K.; Fudo, A. *J. Mol. Catal. A* **2004**, *209*, 9−17. (h) Nomura, K.; Hatanaka, Y.; Okumura, H.; Fujiki, M.; Hasegawa, K. *Macromolecules* **2004**, *37*, 1693−1695. (i) Byun, D. J.; Fudo, A.; Tanaka, A.; Fujiki, M.; Nomura, K. *Macromolecules* **2004**, *37*, 5520−5530. (j) Wang, W.; Tanaka, T.; Tsubota, M.; Fujiki, M.; Yamanaka, S.; Nomura, K. *Adv. Synth. Catal.* **2005**, *347*, 433−446. (k) Wang, W.; Fujiki, M.; Nomura, K. *J. Am. Chem. Soc.* **2005**, *127*, 4582−4583. (l) Nomura, K.; Naga, N.; Miki, M.; Yanagi, K. *Macromolecules* **1998**, *31*, 7588−7597.

(16) Mack, H.; Eisen, M. S. *J. Chem. Soc., Dalton Trans.* **1998**, 917−921.

(17) (a) Thorn, M. G.; Etheridge, Z. C.; Fanwick, P. E.; Rothwell, I. P. *Organometallics* **1998**, *17*, 3636. (b) Thorn, M. G.; Etheridge, Z. C.; Fanwick, P. E.; Rothwell, I. P. *J. Organomet. Chem.* **1999**, *591*, 148.

(18) Fenwick, A. E.; Phomphrai, K.; Thorn, M. G.; Vilardo, J. S.; Trefun, C. A.; Hanna, B.; Fanwick, P. E.; Rothwell, I. P. *Organometallics* **2004**, *23*, 2146−2156.

(19) Virginia, A.; Andrés, R.; Jesús, E. d.; Mata, F. J.; Flores, J. C.; Gómes, R.; Gómes-Sal, P.; Turner, J. F. C. *Organometallics* **2005**, *24*, 2331−2338.

(20) Willoughby, C. A.; Duff, R. R.; Davis, W. M.; Buchwald, S. L. *Organometallics* **1996**, *15*, 472−475.

(21) Zhang, S.; Piers, W. E.; Gao, X. L.; Parvez, M. *J. Am. Chem. Soc.* **2000**, *122*, 5499−5509.

Scheme 2

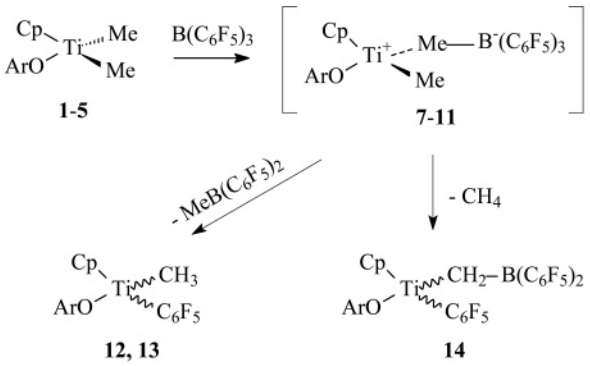

1, **7**; OAr = $OC_6H_3Me_2$-2,6 **2**, **8**; OAr = $OC_6H_3Et_2$-2,6
3, **9**, **12**; OAr = $OC_6H_3{}^iPr_2$-2,6 **4**, **10**, **13**; OAr = $OC_6H_3{}^tBu_2$-2,6
5, **11**, **14**; OAr = OC_6HPh_4-2,3,5,6

at *ortho* positions from **7**−**10**, respectively. The Ti-*Me* carbon atoms of **7**−**10** appeared around 74.7 ppm in the ^{13}C spectrum, significantly downfield from their neutral parent dimethyl complexes (δ 54.0−61.3 ppm). Horton and co-workers suggested that the difference between *meta* and *para* fluorine chemical shifts ($\Delta(m,p$-F)) in the ^{19}F NMR of the $[RB(C_6F_5)_3]^-$ anion can be used to determine the strength of the d^0 metal−anion interaction, where values of 3−6 ppm indicate coordination and values less than 3 ppm indicate noncoordination.[7k] The large $\Delta(m,p$-F) value in the ^{19}F NMR of 5.2−5.4 ppm in **7**−**10** suggested strong association of the $[MeB(C_6F_5)_3]^-$ anion with titanium. At higher temperature, the methyl signals broadened and began to coalesce (ranging from −10 to 15 °C), which was attributed to boron exchange between the two methyl groups on titanium. However, thermal instability of compounds **7**−**10** prevented the detection of a complete coalescence. Only complex **11** was stable enough at higher temperature, and the free energy of activation for this boron exchange was estimated to be 14.4(5) kcal mol^{-1} at 10 °C.[18]

The stability of the cationic compounds is highly dependent on the size of the aryloxide ligand. Larger ligands stabilize the cationic species. For example, a significant deactivation (ca. 20%) of compound **7** (OAr = $OC_6H_3Me_2$-2,6) was observed (^1H NMR) in 15 min at temperatures higher than −20 °C. In contrast, complexes **8**−**11** showed deactivation comparable to that observed by ^1H NMR in 15 min at −10, 10, 10, and 30 °C, respectively. Hence, the order of stability of the cationic complexes is **7** < **8** < **9** ≈ **10** < **11**.

The products from the deactivation of complexes **7**−**11** were identified. Rather than one dominant deactivation pathway (as the case usually is), two deactivation pathways were observed for the same mixed Cp/aryloxide ligand framework (Scheme 2). The first involves exchange of the bridging methyl group (Ti-*Me*-B) with C_6F_5 on boron leading to the neutral complex $CpTi(OAr)(Me)(C_6F_5)$ and $MeB(C_6F_5)_2$. The second is a result of σ-bond metathesis in which a proton on the bridging methyl group (Ti-Me-B) migrates to the terminal methyl (Ti-Me), evolving methane and followed by C_6F_5 transfer to Ti. This deactivation yields complex $CpTi(OAr)(C_6F_5)(CH_2B(C_6F_5)_2)$ as the thermodynamic product. Up to date and to the best of our knowledge, the only example having both deactivation pathways in one complex was reported by Andrés et al. in a related compound, $Cp^*Ti(OSiR_3)Me_2$, activated with $B(C_6F_5)_3$.[19]

Complexes **9** and **10** deactivated rapidly at room temperature, leading to the neutral monomethyl titanium complexes **12** and **13**, respectively, and $MeB(C_6F_5)_2$ via C_6F_5 transfer from the

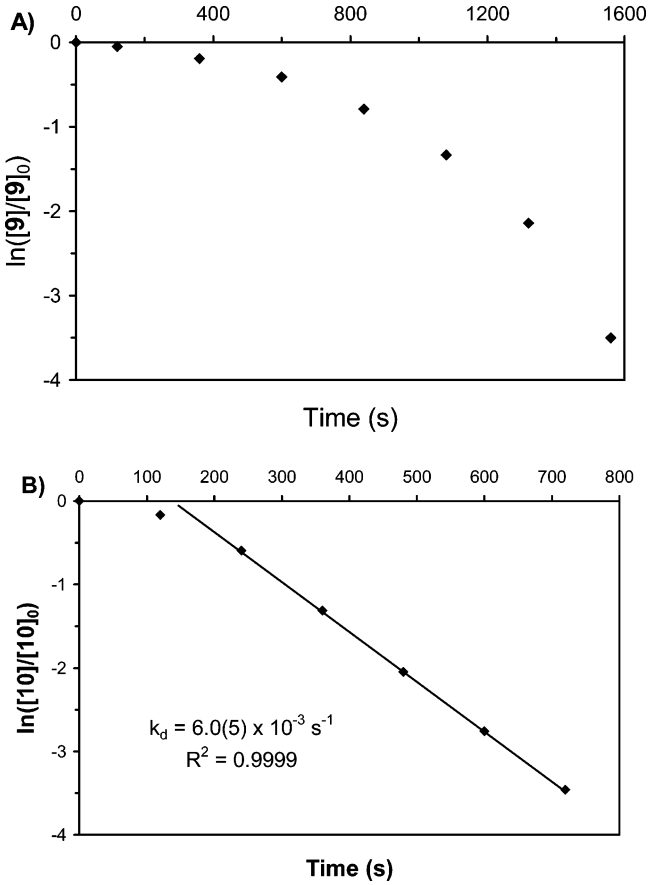

Figure 1. (A) Plot of $\ln([\mathbf{9}]/[\mathbf{9}]_0)$ vs time of the deactivation of $[CpTi(OC_6H_3{}^iPr_2$-2,6)Me$][MeB(C_6F_5)_3]$, **9**, at 10 °C. (B) Plot of $\ln([\mathbf{10}]/[\mathbf{10}]_0)$ vs time of the deactivation of $[CpTi(OC_6H_3{}^tBu_2$-2,6)-Me$][MeB(C_6F_5)_3]$, **10**, at 25 °C. Initial concentrations of **9** and **10** were 0.040 M.

counteranion to the metal.[3,17b,22−24] The deactivation process was monitored by ^1H NMR at 10 and 25 °C following the disappearance of the Cp signal of **9** or **10**, respectively (Figure 1). Despite fairly clean deactivation product, the plot of $\ln([\mathbf{9}]/[\mathbf{9}]_0)$ vs time was rather complicated and deviated significantly from first-order kinetics (Figure 1A). A closer look at the products from the deactivation reaction surprisingly revealed another minor product, $Me_2B(C_6F_5)$. From the deactivation of compound **9** prepared from 1 equiv of **3** and 1 equiv of $B(C_6F_5)_3$, $MeB(C_6F_5)_2$ and $Me_2B(C_6F_5)$ were found at approximately 80 and 20%, respectively. The fact that $Me_2B(C_6F_5)$ was detected in the deactivation reaction implied that $MeB(C_6F_5)_2$ (the primary deactivation product) was also capable of activating $CpTi(OAr)Me_2$ to give $[CpTi(OAr)Me][Me_2B(C_6F_5)_2]$. The secondary deactivation via Me/C_6F_5 exchange then led to compound **12** and $Me_2B(C_6F_5)$. To determine if $Me_2B(C_6F_5)$ was also capable of activating $CpTi(OAr)Me_2$, an excess of compound **3** was allowed to react with $B(C_6F_5)_3$ for several days. Only compound **12** and Me_3B were detected in addition to the starting compound **3**. Formation of Me_3B implied that a similar process in the activation/deactivation of $MeB(C_6F_5)_2$ also occurred for $Me_2B(C_6F_5)$, giving compound **12** and Me_3B as final products. Taking into account that $B(C_6F_5)_3$ is a stronger Lewis acid than $MeB(C_6F_5)_2$ and $Me_2B(C_6F_5)$, reactions of **3** with $MeB(C_6F_5)_2$ and $Me_2B(C_6F_5)$ may not be classified as activation to form cationic species but rather a scrambling of the terminal Me and C_6F_5. A possible reaction scheme is proposed in Scheme 3.

The deactivation of complex **10** at 25 °C was more straightforward, giving only the neutral complex **13** and $MeB(C_6F_5)_2$

Scheme 3

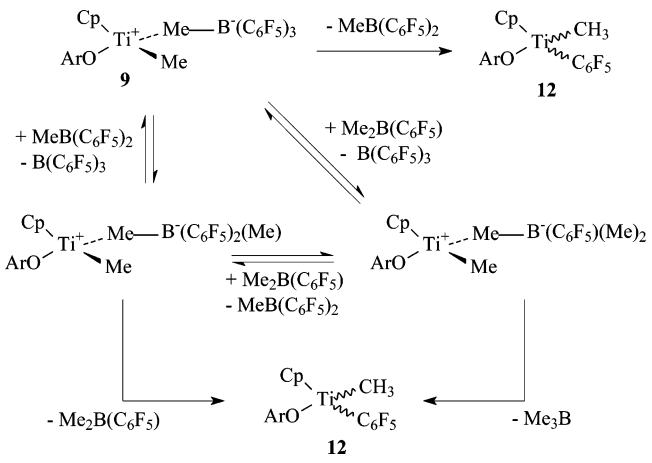

as products. From proton NMR, the formation of $Me_2B(C_6F_5)$, found in the deactivation of **10**, was negligible (<1%). The plot of ln([**10**]/[**10**]$_0$) vs time gave a first-order dependence on [**10**] with a short induction period (Figure 1B). A deactivation rate constant of 6.0(5) $\times$ 10^{-3} s^{-1} at 25 °C was obtained. Preparation of **12** and **13** on a synthetic scale from the reactions of **9** and **10**, respectively, with $B(C_6F_5)_3$ was not successful. Clean products were not recoverable during isolation attempts. The deactivation analysis of cationic compounds **7** and **8** was less conclusive compared to that for compounds **9** and **10** due to multiple deactivation products. However, $MeB(C_6F_5)_2$ was detected in the reaction mixtures, suggesting that the Me/C_6F_5 exchange was one of the deactivation pathways leading to CpTi(OAr)(Me)(C_6F_5).

The second deactivation pathway was observed in the reaction of complex **5** and $B(C_6F_5)_3$. The reaction generated rapidly (^{1}H NMR) the cationic compound **11**, which deactivated to give compound **14**[18] and methane (Scheme 2) via σ-bond metathesis.[7c,18,21,25,26] The deactivation was monitored by ^{1}H NMR following the disappearance of the Cp signal of **11**. The rate of deactivation at various temperatures followed first-order dependence on [**11**]. From the Eyring plot (Figure 2), the activation parameters $\Delta H^{\ddagger}$ = 15.8(5) kcal mol^{-1} and $\Delta S^{\ddagger}$ = −22(5) cal mol^{-1} K^{-1} were obtained. These numbers are comparable to the deactivation of the [Cp*Ti(N=C^{t}Bu$_2$)Me][$MeB(C_6F_5)_3$] system reported by Piers and co-workers, where the deactivation was developed from the contact ion pair rather than two neutral reactants.[21]

Polymerization Studies with 1-Hexene. Polymerizations of 100 equiv of 1-hexene (1.0 M) were conducted using the catalyst precursors **1**−**5** activated with $B(C_6F_5)_3$ in toluene-d_8 at various temperatures. The disappearance of 1-hexene was monitored by ^{1}H NMR following the integrals of the H_2C=C*H*-^{n}Bu proton against CH_2Ph_2 as internal standard. At 25 °C, the cationic titanium complexes **7**−**9** and **11** were active for 1-hexene polymerization. However, thermal instability of complexes **7**−**9** prevented the polymerization from going to completion. The polymerization using **7**−**9** stopped after 40 min at about 60% conversion of monomer, which is in agreement with the observed decomposition of compounds **7**−**9** in the absence of olefin at temperatures higher than 10 °C. Polyhexenes with M_n (PDI) values of 2500 (1.91), 4600 (1.81), and 5000 (1.60) were isolated from the polymerization using **7**−**9**, respectively (Table 1). Compound **10**, on the other hand, generated only a trace amount of polyhexene at any given temperature, possibly as a result of a higher steric encumbrance of the *tert*-butyl groups. Compound **11** rapidly consumed 100 equiv of 1-hexene at 25 °C in 2 min, giving polyhexene with a M_n of 12 100 and a low PDI of 1.14. The fact that the bulky compound **11** is highly active while the ^{t}Bu analogue **10** is inactive seems, at first, puzzling. One possible explanation is that the enhanced reactivity of compound **11** is a result of electron donation (interaction) from the *ortho*-phenyl rings to the titanium center.[27] This interaction effectively reduces the energy barrier required to separate the titanium cation and $[MeB(C_6F_5)_3]^-$ anion, facilitating monomer insertion.

At 0 °C, compounds **7**−**9** were sufficiently stable for complete polymerization of 100 equiv of 1-hexene, giving polyhexene with a M_n (PDI) of 5200 (1.57), 5500 (1.49), and

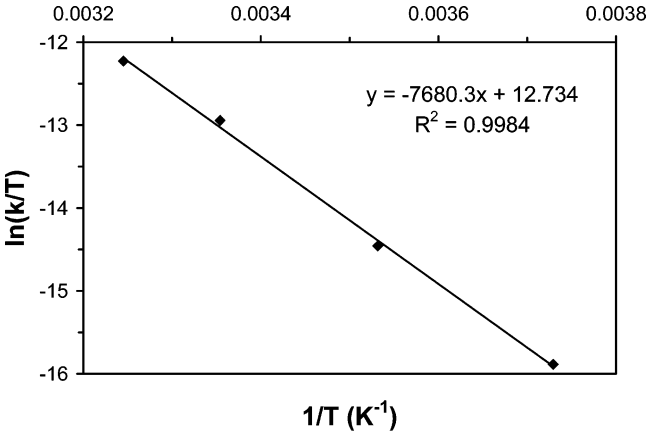

Figure 2. Eyring plot for the deactivation of complex **11** at various temperatures.

Table 1. Polymerization of 100 equiv of 1-Hexene Using Catalyst Precursors 7−11[a]

cat.	temp (°C)	k_{obs} ($\times$ 10^{-4} s^{-1})	act.[b]	M_n	PDI
7	−20	N/A[c]	4.7	4100	1.46
	0	N/A[c]	14	5200	1.57
	25	N/A[d]	9.5	2500	1.91
8	−20	4.4	4.1	4600	1.36
	0	N/A[c]	13	5500	1.49
	25	N/A[d]	24	4600	1.81
9	−20	3.5	3.6	6800	1.24
	0	21	18	6600	1.36
	25	N/A[d]	17	5000	1.60
10	−20		trace		
	0		trace		
	25		trace		
11	−20	52	50	12 600	1.09
	0	N/A[e]	252	12 500	1.10
	25	N/A[e]	504	12 100	1.14

[a] Conditions: Polymerization was carried out using 1.0 M 1-hexene (100 equiv) and 0.010 M [CpTi(OAr)Me][$MeB(C_6F_5)_3$] (1 equiv) in toluene-d_8. [b] Activity: (g polyhexene) (mmol Ti)$^{-1}$ h^{-1} measured when polymerization ceased or at >95% completion. [c] k_{obs} cannot be determined due to a catalyst decomposition. [d] Polymerization ceased at about 60% completion. [e] Polymerization was complete too fast to obtain a reliable k_{obs}. Only activity was reported.

(22) Metcalfe, R. A.; Kreller, D. I.; Tian, J.; Kim, H.; Taylor, N. J.; Corrigan, J. F.; Collins, S. *Organometallics* **2002**, *21*, 1719−1726.
(23) Woodman, T. J.; Thornton-Pett, M.; Bochmann, M. *Chem. Commun.* **2001**, 329−330.
(24) Guerin, F.; Stewart, J. C.; Beddie, C.; Stephan, D. W. *Organometallics* **2000**, *19*, 2994−3000.
(25) Gomez, R.; Gomez-Sal, P.; del Real, P. A.; Royo, P. *J. Organomet. Chem.* **1999**, *588*, 22−27.
(26) Thorn, M. G.; Vilardo, J. S.; Fanwick, P. E.; Rothwell, I. P. *Chem. Commun.* **1998**, 2427−2428.
(27) (a) Lentz, M. R.; Vilardo, J. S.; Lockwood, M. A.; Fanwick, P. E.; Rothwell, I. P. *Organometallics* **2004**, *23*, 329−343. (b) Lentz, M. R.; Fanwick, P. E.; Rothwell, I. P. *Organometallics* **2003**, *22*, 2259−2266. (c) Manz, T. A.; Thomson, K. T., unpublished work.

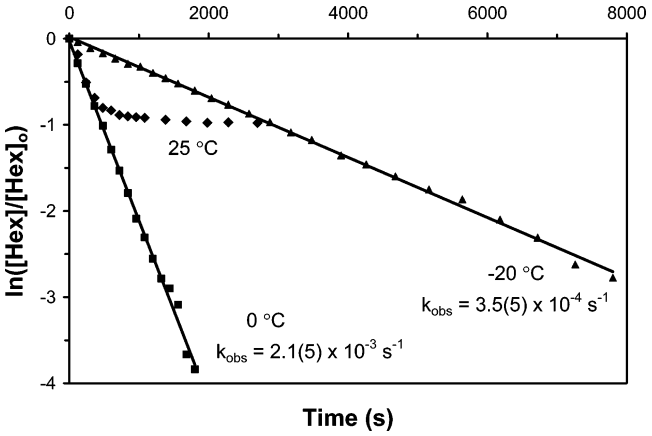

Figure 3. Plot of ln([1-hexene]/[1-hexene]$_0$) vs time for polymerization of 100 equiv of 1-hexene (1.0 M) in toluene-d_8 using [CpTi(OC$_6$H$_3$^{i}Pr$_2$-2,6)Me][MeB(C$_6$F$_5$)$_3$], **9**, at −20, 0, and 25 °C.

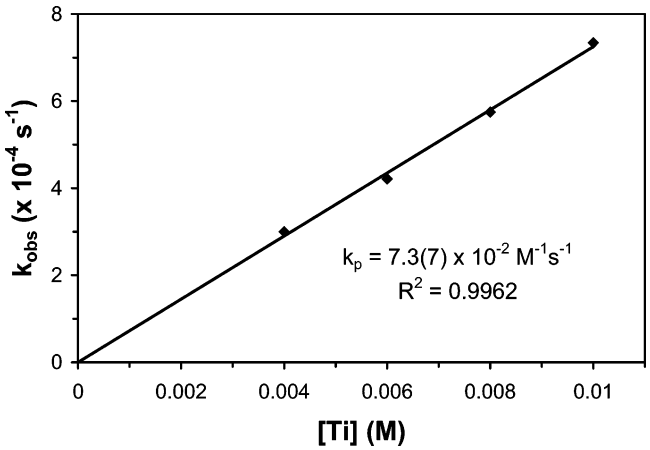

Figure 4. Plot of k_{obs} vs [Ti] of 1-hexene (1.0 M) polymerization at −10 °C using complex **9** at concentrations of 4.0, 6.0, 8.0, and 10.0 mM at 0 °C in toluene-d_8.

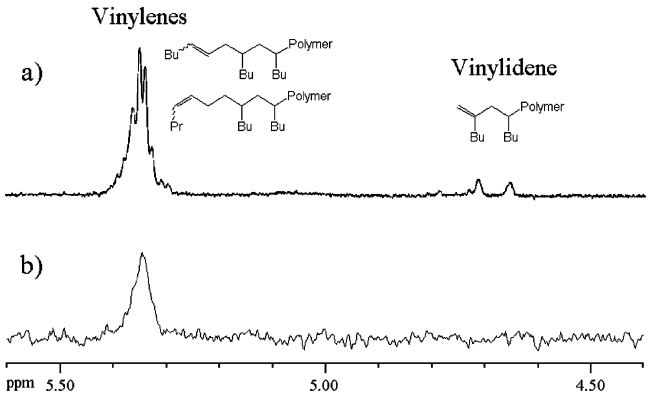

Figure 5. ^{1}H NMR (CDCl$_3$, 300 MHz) spectra of the vinyl region of polyhexene made from (a) complexes **7**−**9** and (b) complex **11**.

6600 (1.36), respectively (Table 1). Although the polymerization using **7** and **8** proceeded to completion, the plot of ln([Hex]/[Hex]$_0$) vs time deviated from linearity, suggesting catalyst deactivation during the course of reaction, which agreed with the observed instability of **7** and **8** at 0 °C. As illustrated in Figure 3, the catalyst generated from complex **9** at 0 °C was persistent during the polymerization reaction, giving pseudo-first-order dependence on [1-hexene] with a k_{obs} of 2.1(5) × 10^{-3} s^{-1}. Compound **11** still consumed 100 equiv of 1-hexene rapidly at 0 °C in 4 min, giving polyhexene with a M_n of 12 500 and a low PDI of 1.10.

At −20 °C, polyhexene with M_n (PDI) values of 4100 (1.46), 4600 (1.36), 6800 (1.24), and 12 600 (1.09) was isolated from the polymerization using **7**−**9** and **11**, respectively (Table 1). Only the polymerization using **8**, **9**, and **11** was pseudo-first-order dependent on [1-hexene] with a k_{obs} of 4.4(5) × 10^{-4}, 3.5(5) × 10^{-4}, and 5.2(5) × 10^{-3} s^{-1}, respectively, in agreement with their stability at −20 °C. With the exception of complex **11**, the polymerization rate decreased with increasing bulk of the aryloxide ligand. With a given catalyst, higher PDI and higher polymerization rate were observed with increasing temperature. At a given temperature, higher PDI was observed in the order **11** < **9** < **8** < **7** and higher M_n in the reverse order **7** < **8** < **9** < **11**. This is understandable in terms of steric hindrance at titanium, where steric encumbrance and lower temperature suppress chain termination/transfer processes such as β-H elimination.

Polymerizations of 1-hexene (1.0 M) were carried out at −10 °C in toluene-d_8 using various concentrations of **9**. The polymerizations were first-order dependent on [1-hexene] for [Ti] = 4.0, 6.0, 8.0, and 10.0 mM. A plot of k_{obs} vs Ti concentrations revealed a linear dependence on catalyst, in agreement with the rate law: $-d[1\text{-hexene}]/dt = k_p[Ti][1\text{-hexene}]$ for the case where there was no catalyst decomposition (Figure 4). From the plot, k_p = 7.3(7) × 10^{-2} M^{-1} s^{-1} at −10 °C was obtained.

By comparison to the related Cp′Ti(OAr)Me$_2$ and Cp′Ti(OAr)Cl$_2$ catalyst systems investigated by Nomura and coworkers, our CpTi(OAr)Me$_2$/B(C$_6$F$_5$)$_3$ system is less reactive for 1-hexene polymerization by an order of magnitude.[15e,l] The important contributor to the activity difference is the activator/cocatalyst (such as MAO, AlR$_3$, [Ph$_3$CB][(C$_6$F$_5$)$_4$], or [Me$_2$PhNHB][(C$_6$F$_5$)$_4$]) used in Nomura's system. These activators generally yield highly efficient olefin polymerization catalysts, while B(C$_6$F$_5$)$_3$ tends to afford less effective catalysts.[4] However, one of the advantages of using B(C$_6$F$_5$)$_3$ is a lower activity catalyst that is amenable to kinetic investigations.

On the basis of ^{13}C{^{1}H} NMR in CDCl$_3$, the polyhexene produced from every catalyst precursor at every temperature was atactic polyhexene.[28,29] ^{1}H NMR of polyhexene is very informative especially in the range δ 4.50−5.50 ppm.[30] The ^{1}H NMR spectra of polyhexene produced from **7**−**9** were very similar in both shape and intensity. Therefore, only NMR data from **9** are shown in Figure 5a. There were only two signals observed in this region at about 4.70 and 5.35 ppm, which corresponded to the vinylidene and vinylene end groups, respectively. These unsaturated end groups are common in olefin polymerization using group 4 metal complexes. The vinylidene and vinylene end groups are typically formed during the polymerization as a result of β-H elimination following a 1,2- and 2,1-insertion of 1-hexene, respectively. The presence of both end groups in polyhexene produced from **7**−**9** suggested that β-H elimination occurred after both 1,2- and 2,1-insertion of 1-hexene. As shown in Figure 5a, the vinylene end group was formed about 10 times more than the vinylidene end group. The relative amount of the vinylidene and vinylene end groups did not change significantly in the polymerization at −20, 0, or 25 °C. The proton NMR of polyhexene produced from the bulkier complex **11** is also shown in Figure 5b. There was only

(28) Asakura, T.; Demura, M.; Nishiyama, Y. *Macromolecules* **1991**, *24*, 2334−2340.
(29) Murray, M. C.; Baird, M. C. *Can. J. Chem.* **2001**, *79*, 1012−1018.
(30) Liu, Z.; Somsook, E.; White, C. B.; Rosaaen, K. A.; Landis, C. R. *J. Am. Chem. Soc.* **2001**, *123*, 11193−11207.

one signal observed at about 5.35 ppm, which corresponded to the vinylene end group. This suggested that the polymer chain termination occurred only after the 2,1-misinsertion, but not after the regular 1,2-insertion. The more hindered aryloxide and the interaction of phenyl groups with the titanium center in **11** could be responsible for the prevention of chain termination after regular 1,2-insertion of 1-hexene. This is in agreement with the observed high M_n and low PDI in polyhexene produced from **11**. The vinylene end group was observed exclusively in the polymerization using **11** at every measured temperature.

Conclusions

We have demonstrated herein the use of aryloxides as ancillary ligands in the study of activation, deactivation, and 1-hexene polymerization with titanium dimethyl complexes. We have identified two different deactivation pathways. The cationic titanium complexes have been shown to be active for 1-hexene polymerization at −20, 0, and 25 °C, giving atactic polyhexene. The titanium cationic catalyst stability and polymerization rates depend strongly on the aryloxide ligand. Bulkier aryloxide is more stable but less active for 1-hexene polymerization. The exception is OC_6HPh_4-2,3,5,6, where the *ortho*-phenyl rings facilitate monomer coordination, giving rise to an increased polymerization rate. This effect is being scrutinized in more detail.

Experimental Section

General Details. All operations were carried out under dry nitrogen atmosphere using standard Schlenk techniques. Hydrocarbon solvents were purified using an Innovative Technologies solvent purification system and were stored over sodium ribbons under nitrogen until use. LiMe (Aldrich), $B(C_6F_5)_3$ (Strem), and 2,6-diethylphenol (Ethyl Corp.) were used as received. Compounds **1**, **3**, **5**,[18] and $CpTi(OC_6H_3{}^tBu_2\text{-}2,6)Cl_2$[20] were prepared according to literature procedures. ^1H and ^{13}C NMR spectra were recorded on a Varian Associates Gemini-200 or Inova-300 spectrometer and referenced to protio impurities of commercial benzene-d_6 (C_6D_6), chloroform-d ($CDCl_3$), or toluene-d_8 (C_7D_8) as internal standards. Elemental analyses and X-ray crystallography were obtained through Purdue in-house facilities. Gel permeation chromatography (GPC) was performed using a Waters 1515 isocratic HPLC pump running at a THF flow rate of 1 mL/min at 35 °C and a Waters 2414 refractive index detector to determine molecular weights and molecular weight distributions of polymer samples with respect to polystyrene standards.

$CpTi(OC_6H_3Et_2\text{-}2,6)Me_2$, 2. LiMe (9.0 mL, 1.6 M solution in diethyl ether, 14 mmol) was added dropwise to a precooled suspension of $CpTiCl_3$ (1.00 g, 4.56 mmol) in 30 mL of Et_2O at −78 °C. After the mixture was stirred for approximately 4 h at −78 °C, a solution of 2,6-diethylphenol (0.684 g, 4.56 mmol) in 10 mL of Et_2O was added dropwise. The mixture was slowly warmed to room temperature and stirred overnight. The solvent was then removed under vacuum, and benzene was added to the solid residue. The suspension was filtered through a plug of Celite over fritted glass to remove the lithium salts. The filtrate was evacuated to dryness, yielding a dark yellow liquid. Upon standing at room temperature for a few hours, the liquid solidified, giving a dark yellow solid (1.04 g, 78%). The solid was stored at −30 °C to prevent decomposition. Anal. Calcd for $C_{17}H_{24}OTi$: C, 69.91; H, 8.22. Found: C, 69.26; H, 8.14. ^1H NMR (C_6D_6, 25 °C): δ 7.03 (d, $J = 7.5$ Hz, 2H, *m*-H); 6.93 (t, $J = 7.5$ Hz, 1H, *p*-H); 5.87 (s, 5H, Cp); 2.59 (quartet, $J = 7.5$ Hz, 4H, CH_2CH$_3$); 1.21 (t, $J = 7.5$ Hz, 6H, CH$_2$CH_3); 0.91 (s, 6H, Ti-Me). ^{13}C NMR (C_6D_6, 25 °C): δ 163.1 (Ti−O-*C*); 134.1, 127.2, 122.5 (Ar-*C*); 114.4 (Cp); 54.5 (Ti-*Me*); 24.7 (*C*H$_2$CH$_3$); 15.5 (CH$_2$*C*H$_3$).

$CpTi(OC_6H_3{}^tBu_2\text{-}2,6)Me_2$, 4. LiMe (3.2 mL, 1.6 M solution in diethyl ether, 5.1 mmol) was added to a chilled solution (10 °C) of $CpTi(OC_6H_3{}^tBu_2\text{-}2,6)Cl_2$ (1.00 g, 2.57 mmol) in 20 mL of benzene. The mixture was slowly warmed to room temperature in 30 min and stirred for 2 h. The solvent was then removed under vacuum, and hexane was added to the solid residue. The suspension was filtered through a plug of Celite over fritted glass to remove the lithium salts. The filtrate was then evacuated to dryness, giving a dark yellow solid (0.81 g, 91%). Anal. Calcd for $C_{21}H_{32}OTi$: C, 72.46; H, 9.19. Found: C, 72.21; H, 9.13. ^1H NMR (C_6D_6, 25 °C): δ 7.30 (d, $J = 7.8$ Hz, 2H, *m*-H); 6.90 (t, $J = 7.8$ Hz, 1H, *p*-H); 5.90 (s, 5H, Cp); 1.41 (s, 18H, ^{t}Bu); 1.02 (s, 6H, Ti-Me). ^{13}C NMR (C_6D_6, 25 °C): δ 166.5 (Ti−O-*C*); 139.8, 125.5, 121.0 (Ar-*C*); 114.9 (Cp); 61.3 (Ti-*Me*); 35.5 (*C*Me$_3$); 31.6 (C*Me*$_3$).

NMR-Scale Synthesis of $[CpTi(OC_6H_3Me_2\text{-}2,6)Me][MeB(C_6F_5)_3]$, 7. The following synthesis of **7** was also used to synthesize complexes **8**−**10**. An NMR tube with a rubber-septum screw cap was charged with $CpTi(OC_6H_3Me_2\text{-}2,6)Me_2$ (10 mg, 40 μmol) and 0.30 mL of toluene-d_8. A solution of $B(C_6F_5)_3$ in toluene-d_8 (0.20 mL, 0.20 M, 40 μmol) was added to the NMR tube through the rubber septum at −25 °C, giving a bright red solution of compound **7**. ^1H NMR (C_7D_8, −25 °C): δ 6.68 (m, 3H, *m*, *p*-H); 5.50 (s, 5H, Cp); 1.67 (s, 6H, *o*-Me); 1.51 (s, 3H, Ti-*Me*); 0.64 (br, 3H, B-*Me*). Selected ^{13}C NMR (C_7D_8, −25 °C): δ 165.2 (Ti-O-*C*); 119.1 (Cp); 75.2 (Ti-*Me*). ^{19}F NMR (C_7D_8, −25 °C): δ −134.6 (d, 6F, *o*-F); −159.4 (t, 3F, *p*-F); −164.8 (m, 6F, *m*-F).

$[CpTi(OC_6H_3Et_2\text{-}2,6)Me][MeB(C_6F_5)_3]$, 8. ^1H NMR (C_7D_8, −25 °C): δ 6.84 (t, $J = 6.9$ Hz, 1H, *p*-H); 6.77 (d, $J = 6.9$ Hz, 2H, *m*-H); 5.55 (s, 5H, Cp); 2.08 (quartet, $J = 7.5$ Hz, 4H, CH_2-CH$_3$); 1.57 (s, 3H, Ti-*Me*); 0.95 (t, $J = 7.5$ Hz, 6H, CH$_2$CH_3); 0.77 (br, 3H, B-*Me*). Selected ^{13}C NMR (C_7D_8, −25 °C): δ 164.4 (Ti-O-*C*); 119.3 (Cp); 75.2 (Ti-*Me*). ^{19}F NMR (C_7D_8, −25 °C): δ −134.8 (d, 6F, *o*-F); −159.4 (t, 3F, *p*-F); −164.8 (m, 6F, *m*-F).

$[CpTi(OC_6H_3{}^iPr_2\text{-}2,6)Me][MeB(C_6F_5)_3]$, 9. ^1H NMR (C_7D_8, −25 °C): δ 6.81 (m, 3H, *m*, *p*-H); 5.60 (s, 5H, Cp); 2.63 (m, $J =$ 6.6 Hz, 2H, C*H*Me$_2$); 1.61 (s, 3H, Ti-*Me*); 1.01 (d, $J = 7.2$ Hz, 6H, CH*Me*$_2$); 0.88 (d, $J = 7.2$ Hz, 6H, CH*Me*$_2$); 0.84 (br, 3H, B-*Me*). Selected ^{13}C NMR (C_7D_8, −25 °C): δ 162.9 (Ti-O-*C*); 119.2 (Cp); 75.2 (Ti-*Me*). ^{19}F NMR (C_7D_8, −25 °C): δ −134.8 (d, 6F, *o*-F); −159.3 (t, 3F, *p*-F); −164.7 (m, 6F, *m*-F).

$[CpTi(OC_6H_3{}^tBu_2\text{-}2,6)Me][MeB(C_6F_5)_3]$, 10. ^1H NMR (C_7D_8, −25 °C): δ 7.01 (d, $J = 6.9$ Hz, 2H, *m*-H); 6.73 (t, $J = 6.9$ Hz, 1H, *p*-H); 5.70 (s, 5H, Cp); 1.76 (s, 3H, Ti-*Me*); 0.98 (br, 18H, ^{t}Bu); 0.86 (br, 3H, B-*Me*). Selected ^{13}C NMR (C_7D_8, −25 °C): δ 168.6 (Ti−O-*C*); 120.8 (Cp); 75.2 (Ti-*Me*). ^{19}F NMR (C_7D_8, −25 °C): δ −134.4 (d, 6F, *o*-F); −159.6 (t, 3F, *p*-F); −164.8 (m, 6F, *m*-F).

NMR-Scale Synthesis of $CpTi(OC_6H_3{}^iPr_2\text{-}2,6)Me(C_6F_5)$, 12. Compound **9** was generated in situ from compound **3** and $B(C_6F_5)_3$ in an NMR tube. The NMR tube was left at room temperature for 3 h, during which time the color slowly changed from red to yellow, giving compounds **12**, $MeB(C_6F_5)_2$, and $Me_2B(C_6F_5)$. ^1H NMR (C_7D_8, 25 °C): δ 6.50−7.20 (m, 3H, *m*, *p*-H); 6.12 (s, 5H, Cp); 3.44 (m, $J = 6.9$ Hz, 2H, C*H*Me$_2$); 1.47 (m, $^5J_{HF} = 1.9$ Hz, Ti-*Me*); 1.15 (d, $J = 6.9$ Hz, 6H, CH*Me*$_2$); 1.12 (d, $J = 6.9$ Hz, 6H, CH*Me*$_2$). Selected ^{13}C NMR (C_7D_8, 25 °C): δ 162.5 (Ti-O-*C*); 117.1 (Cp); 74.7 (Ti-*Me*). ^{19}F NMR (C_7D_8, 25 °C): δ −117.5 (m, 2F, *o*-F); −155.2 (m, 1F, *p*-F); −163.0 (m, 2F, *m*-F).

NMR-Scale Synthesis of $CpTi(OC_6H_3{}^tBu_2\text{-}2,6)Me(C_6F_5)$, 13. Compound **10** was generated in situ from compound **4** and $B(C_6F_5)_3$ in an NMR tube. The NMR tube was left at room temperature for 3 h, during which time the color slowly changed from red to yellow, giving compounds **13** and $MeB(C_6F_5)_2$. ^1H NMR (C_7D_8, 25 °C): δ 7.13 (d, $J = 7.0$ Hz, 2H, *m*-H); 6.79 (t, $J = 7.0$ Hz, 1H, *p*-H); 6.13 (s, 5H, Cp); 1.58 (m, 3H, Ti-*Me*); 1.18 (s, 18H, ^{t}Bu). ^{19}F NMR (C_7D_8, 25 °C): δ −115.7 (m, 2F, *o*-F); −154.9 (m, 1F, *p*-F); −163.3 (m, 2F, *m*-F).

Deactivation Studies of Compounds 9−11. The following representative deactivation study of **9** was also used for **10** and **11**. Ph_2CH_2 (2 μL) was added to a solution of **3** in toluene-d_8 (0.30 mL, 0.067 M, 20 μmol) in a screw-cap NMR tube with a PTFE/silicone septum. This solution was then cooled to 10 °C using a cooler attached to the NMR spectrometer. An NMR spectrum was acquired. This is taken as the spectrum at time = 0 s. The sample was taken out of the spectrometer and submerged in a 10 °C water bath. A solution of $B(C_6F_5)_3$ in toluene-d_8 (0.20 mL, 0.10 M, 20 μmol) was then added through the septum. The NMR tube was shaken vigorously and placed back immediately into the spectrometer. The initial concentrations of **9** and Ph_2CH_2 were 0.040, and 0.024 M, respectively. The formation of **12** was monitored by ^{1}H NMR with integration against the internal standard Ph_2CH_2. Deactivation studies of **10** were performed similarly at 25 °C. A deactivation study of **11** was performed at −5, 10, 25, and 35 °C.

NMR-Scale Polymerization of 1-Hexene. The following representative polymerization of 1-hexene at 0 °C was used for all catalysts at −20, 0, and 25 °C. A solution of the catalyst precursor in toluene-d_8 (50.0 μL, 0.10 M, 5.0 μmol) was added to a mixture of 1-hexene (62.5 μL, 0.500 mmol) and Ph_2CH_2 (10 μL) in 0.34 mL of toluene-d_8 in a screw-cap NMR tube with a PTFE/silicone septum. This solution was then cooled to 0 °C using a cooler attached to the NMR spectrometer. An NMR spectrum was taken. This is the spectrum at time = 0 s. A solution of $B(C_6F_5)_3$ in toluene-d_8 (50.0 μL, 0.10 M, 5.0 μmol) was then added through a septum at 0 °C. The NMR tube was shaken vigorously and quickly placed back into the spectrometer. The initial concentrations of 1-hexene, $[CpTi(OAr)Me][MeB(C_6F_5)_3]$, and Ph_2CH_2 were 1.0, 0.010, and 0.12 M, respectively. The conversion of 1-hexene was monitored by proton NMR integration against the internal standard Ph_2CH_2. After the polymerization proceeded to over 95% completion, the solution was poured into excess methanol to precipitate the polymer. The excess methanol was decanted, and the polymer was dried under vacuum overnight.

Acknowledgment. Support for this research was provided by the U.S. Department of Energy, Office of Basic Energy Sciences, through the Catalysis Science Grant No. DE-FG02-03ER15466.

Supporting Information Available: Synthesis, ORTEP drawing, and X-ray crystallographic data (CIF file) for compound **6**. This material is available free of charge via the Internet at http://pubs.acs.org.

OM0507272